

# ***Chemistry R & D for Back End Fuel Cycle for Fast Reactors in India***



**P.R.Vasudeva Rao**



***Indira Gandhi Centre for Atomic Research  
Kalpakkam  
vasu@igcar.gov.in***

Global2011  
13 Dec.2011

# FBR Evolution in India

Credible confidence in fuel cycle

25 years of successful operation

State-of-art concepts

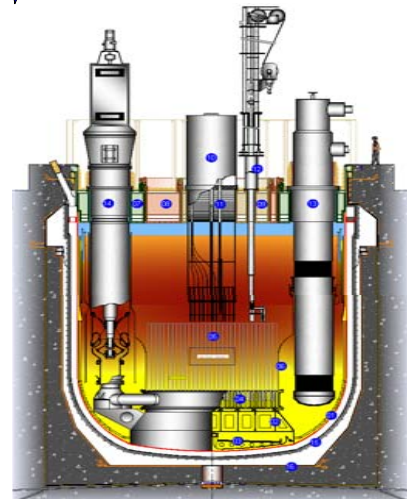
Innovative concepts

Human resources



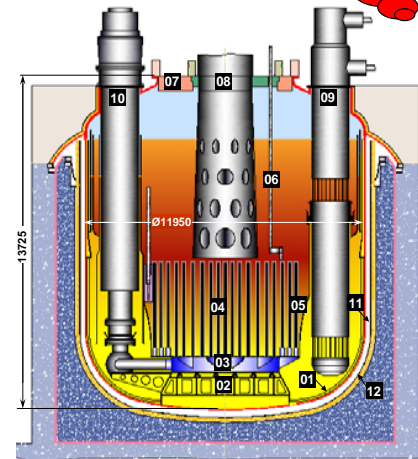
## **FBTR**

- 40 MWt (13.5 MWe)
- Loop type reactor
- PuC – UC
- Design: CEA, France
- Since 1985...



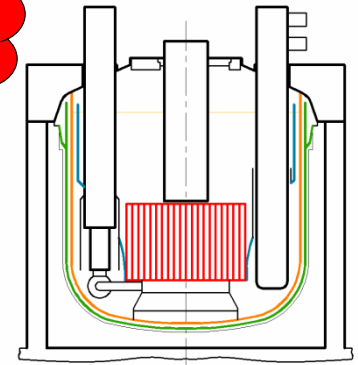
## **PFBR**

- 1250 MWt (500 MWe)
- Pool Type
- UO<sub>2</sub>-PuO<sub>2</sub>
- Indigenous design and construction
- To be commissioned in 2012



## **CFBR**

- 500 MWe
- Pool Type
- UO<sub>2</sub>-PuO<sub>2</sub>
- Six units (3 twin units)
- To be commissioned around 2023



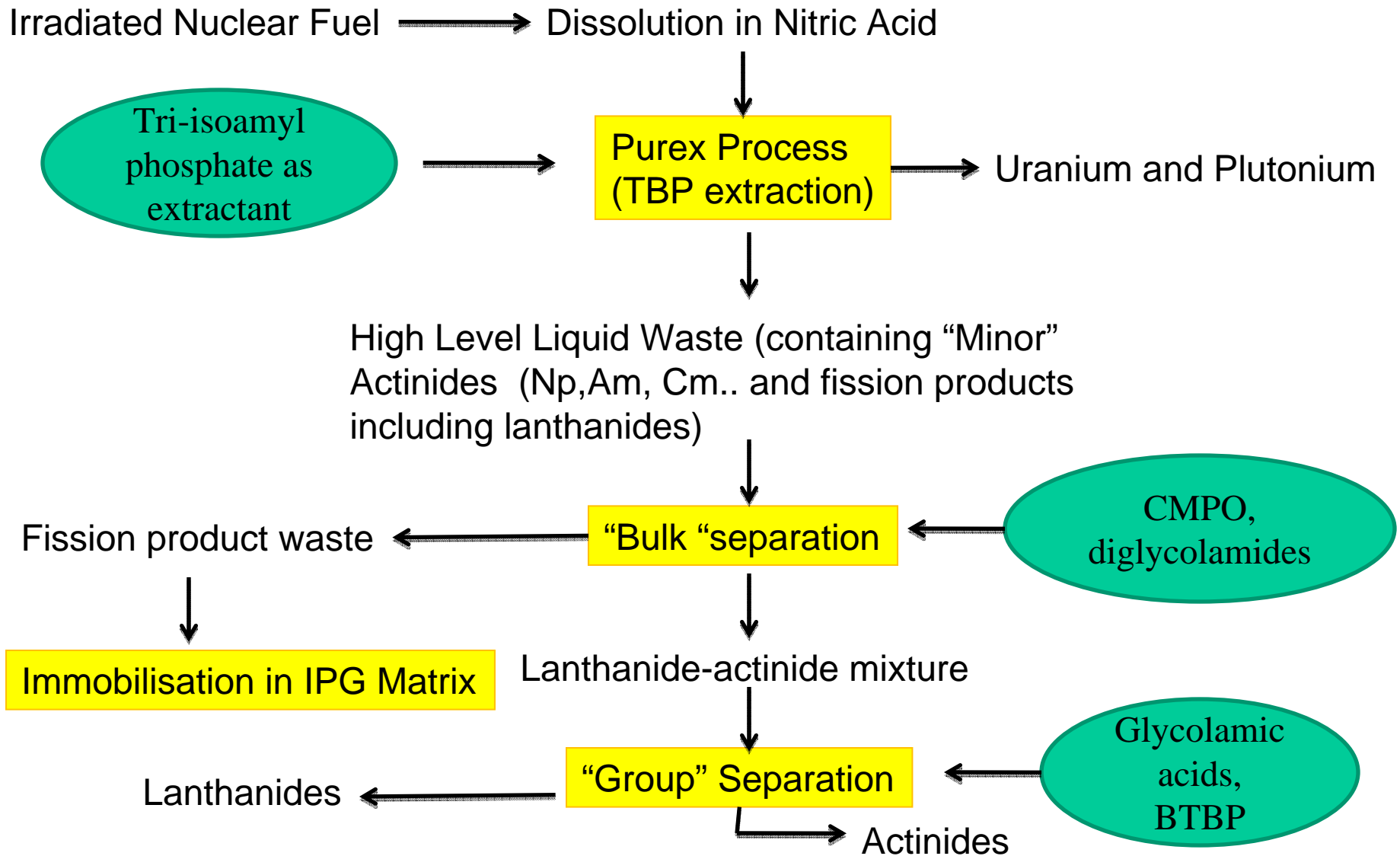
## **Future FBR**

- 1000 MWe
- Pool Type
- Metallic fuel
- Serial construction
- Beyond 2025

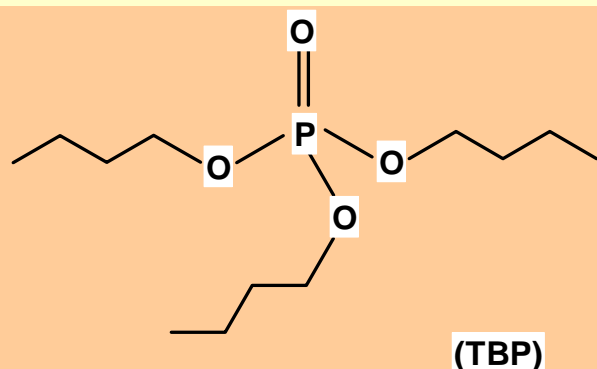
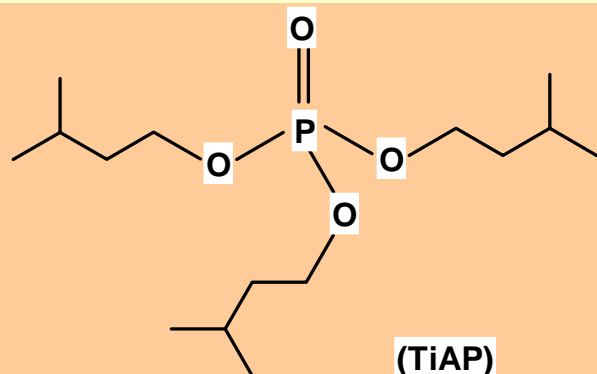
# Fast Reactor Fuels in India

Fuel		Pu content (Pu/(U+Pu))	Reactor	Remarks
Uranium, plutonium mixed carbide	(U,Pu)C	0.7 /0.55	FBTR	Fuel has reached a burn-up of 162 GWd/t; fuel discharged upto 150 GWD/T has been reprocessed; fuel fabricated from Pu recovered and loaded in FBTR
Uranium, plutonium mixed oxide	(U,Pu)O <sub>2</sub>	0.21 / 0.28	PFBR	Test fuel has reached burn-up of 112 GWd/t in FBTR; PIE under progress
Uranium, plutonium- zirconium metal alloy	U-Pu-Zr	0.19	Future FBRs	Sodium bonded U-Zr fuel pins under irradiation in FBTR; pyroprocessing under development

# Reprocessing and Waste Management



# Comparison of Tri-n-butyl phosphate (TBP) and Tri-iso-amyl phosphate (TiAP)



Extraction and stripping behaviour of TiAP is comparable to that of TBP.

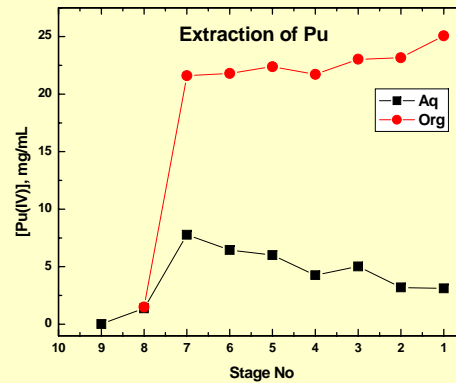
TiAP has high capacity to load tetravalent metal ions such as Pu(IV) and Th(IV) without third phase formation.

Its radiation stability is at par with that of TBP.

Property		Extractant	
		TBP	TiAP
Molecular Weight (g/mol)		266.3	308.4
Density of TalP at 298 K (g/cc)	Dry	0.976	0.948
	WS	0.980	0.952
Density of 1.1M TalP/n-DD at 298 K (g/cc)		0.812	0.812
Solubility of water in TalP at 298 K (mg H <sub>2</sub> O/mL WS TalP)		67.0	41.1
Aqueous solubility of TalP at 298 K (mg TalP/ℓ water)		388	< 100
[HNO <sub>3</sub> ] <sub>org</sub> in equilibrium with 4M HNO <sub>3</sub> for 1.1M TalP/n-DD in the absence of metal ions at 303 K (mol/ℓ)		0.824	0.810
$D_{U(V)}$ from nitric acid media by 1.1M TalP/n-DD at 303 K	0.01M HNO <sub>3</sub>	0.01	0.011
	4M HNO <sub>3</sub>	30.9	35.2
$D_{Pu(IV)}$ from nitric acid media by 1.1M TalP/n-DD at 303 K	0.5M HNO <sub>3</sub>	0.81	0.90
	4M HNO <sub>3</sub>	24.1	29.3
LOC for TPF at 303 K (mg/mL) in 1.1M TalP / n-DD – Th(NO <sub>3</sub> ) <sub>4</sub> – 3M HNO <sub>3</sub> system		40.1	75.6
LOC for TPF at 303 K (mg/mL) in 1.1M TalP / n-DD – Pu(NO <sub>3</sub> ) <sub>4</sub> – 3M HNO <sub>3</sub> system		~ 60	No TPF under similar conditions. ~ 120 g/ℓ can be loaded.

- TalP: Trialkyl Phosphate; WS: Water Saturated;
- LOC: Limiting Organic Concentration; TPF: Third Phase Formation

# Demonstration of Feasibility of using TiAP as an Alternate Extractant in FRFR

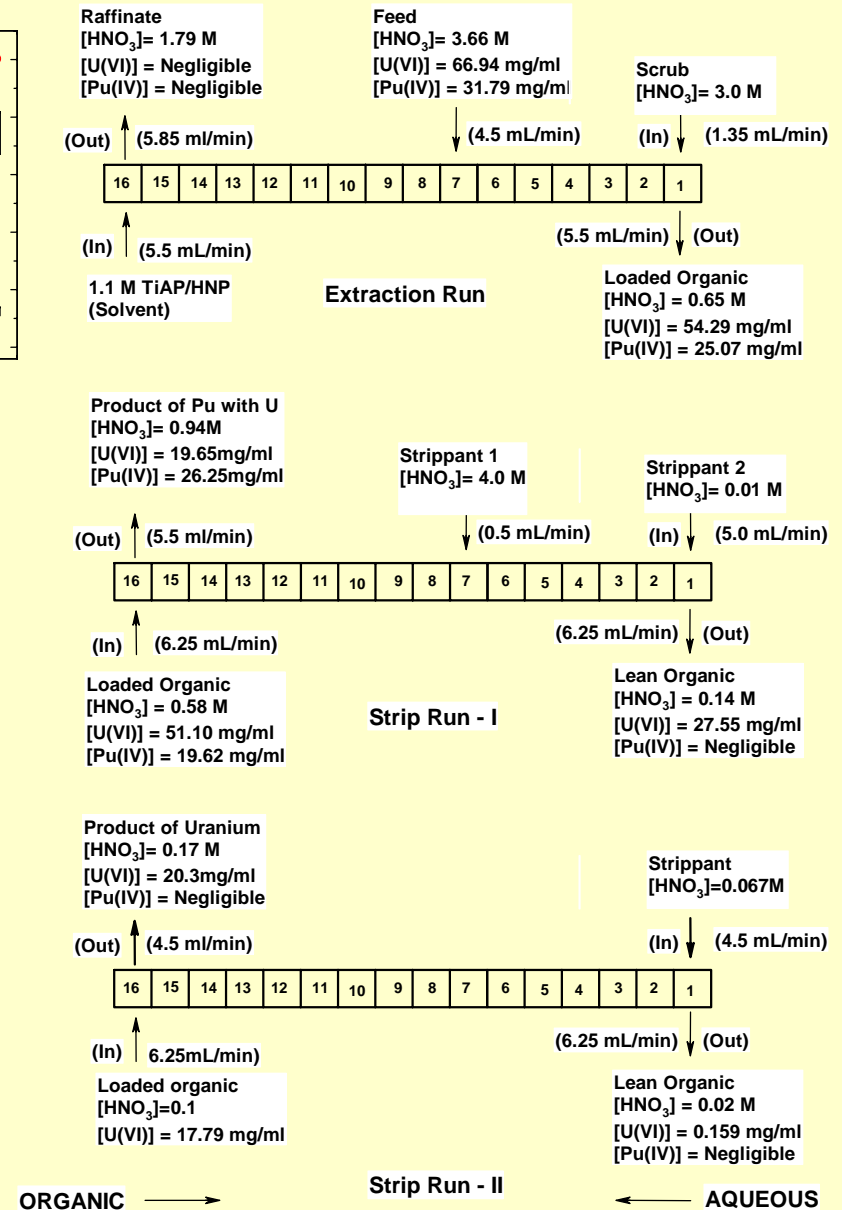


TiAP extraction study:

Feed: U 67 mg/ml, Pu 32 mg/ml in 3.7 M nitric acid  
U and Pu quantitatively extracted and stripped.

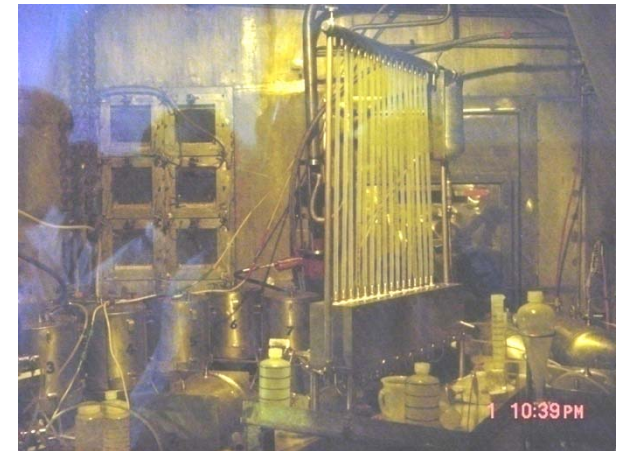
## Future studies planned :

- 1) U(VI) extraction by 1.1 M TiAP/HNP under high solvent loading conditions to understand the hydrodynamics of the system for extreme conditions.
- 2) Solvent recycling.
- 3) Extraction of heavy metals in the presence of FPs – to establish the DFs achievable in TiAP system.



# Bulk separation of Minor Actinides and Lanthanides from High Active Liquid Waste

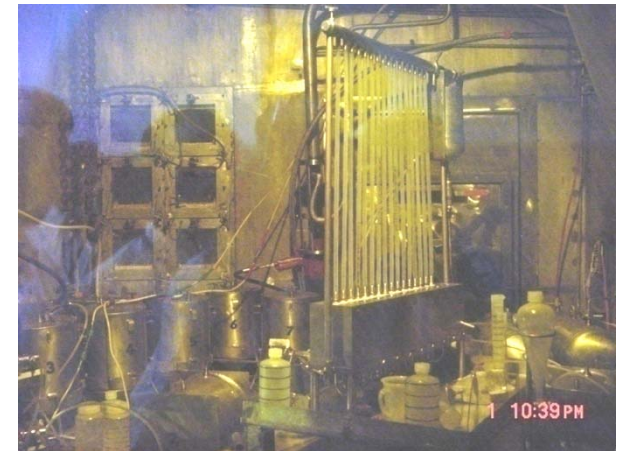
*Objective: To develop a process for bulk separation of An and Ln from HLW, and subsequent separation of An from Ln, by compatible processes*



# Bulk separation of Minor Actinides and Lanthanides from High Active Liquid Waste

*Objective: To develop a process for bulk separation of An and Ln from HLW, and subsequent separation of An from Ln, by compatible processes*

- HAW (155 GWd/Te) was characterized by various analytical techniques.

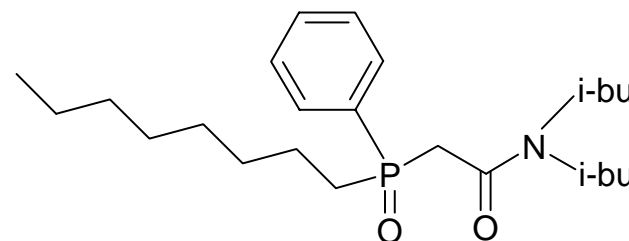
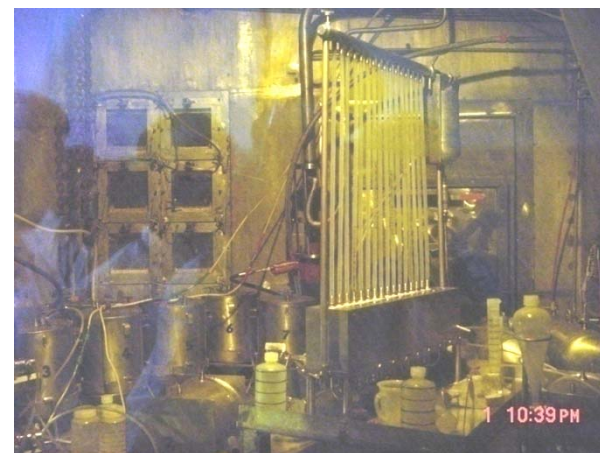




# Bulk separation of Minor Actinides and Lanthanides from High Active Liquid Waste

**Objective:** To develop a process for bulk separation of An and Ln from HLW, and subsequent separation of An from Ln, by compatible processes

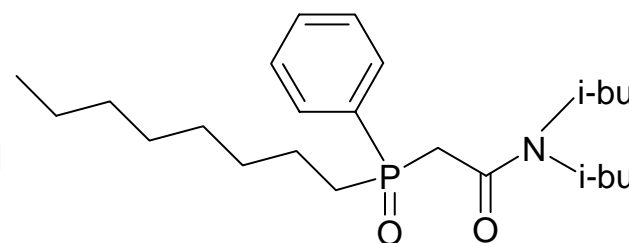
- HAW (155 GWd/Te) was characterized by various analytical techniques.
- Demonstration run in hot cells
  - Quantitative separation and recovery (>99%) of trivalents (Am(III)+ Ln (III)) from HAW using 0.2 M CMPO-1.2 M TBP
  - Extraction in 5-6 stages; Stripping in 10-12 stages

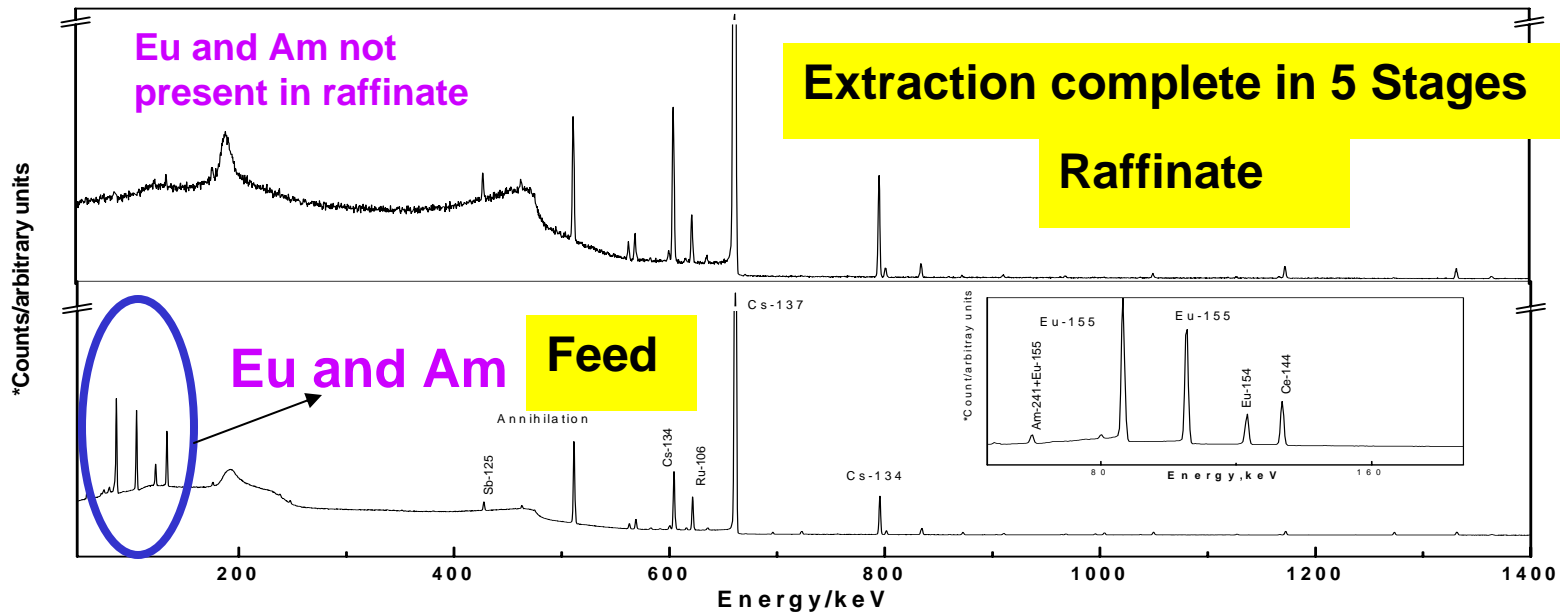


# Bulk separation of Minor Actinides and Lanthanides from High Active Liquid Waste

**Objective:** To develop a process for bulk separation of An and Ln from HLW, and subsequent separation of An from Ln, by compatible processes

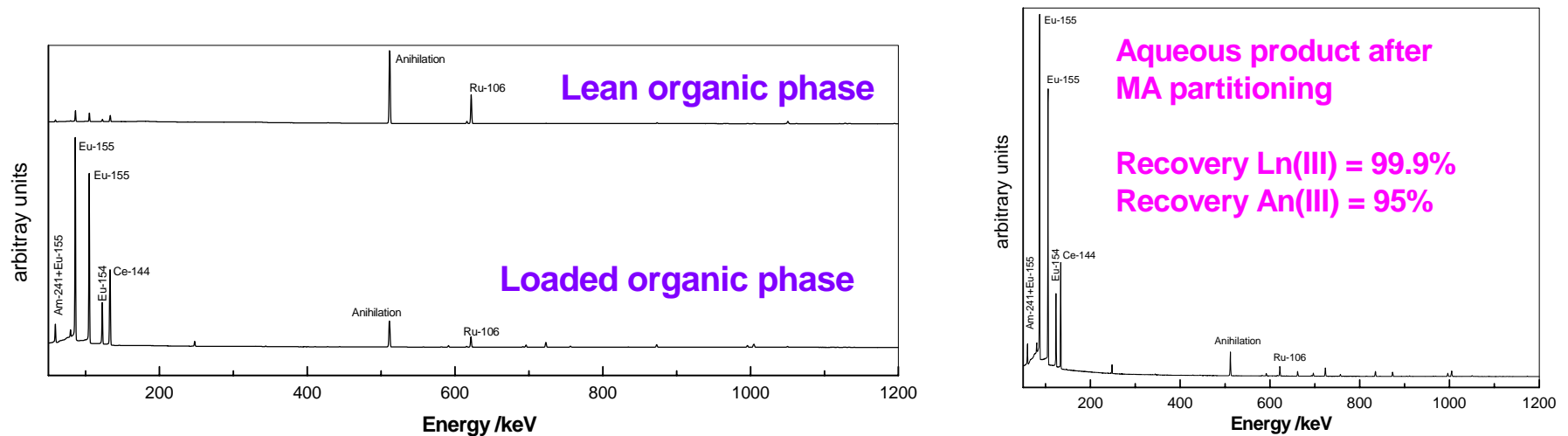
- HAW (155 GWd/Te) was characterized by various analytical techniques.
- Demonstration run in hot cells
  - Quantitative separation and recovery (>99%) of trivalents (Am(III)+ Ln (III)) from HAW using 0.2 M CMPO-1.2 M TBP
  - Extraction in 5-6 stages; Stripping in 10-12 stages
- Nearly 20 – 25 % of radioruthenium was carried to lean organic
  - Decontaminated with sodium hydroxide or sodium carbonate solutions

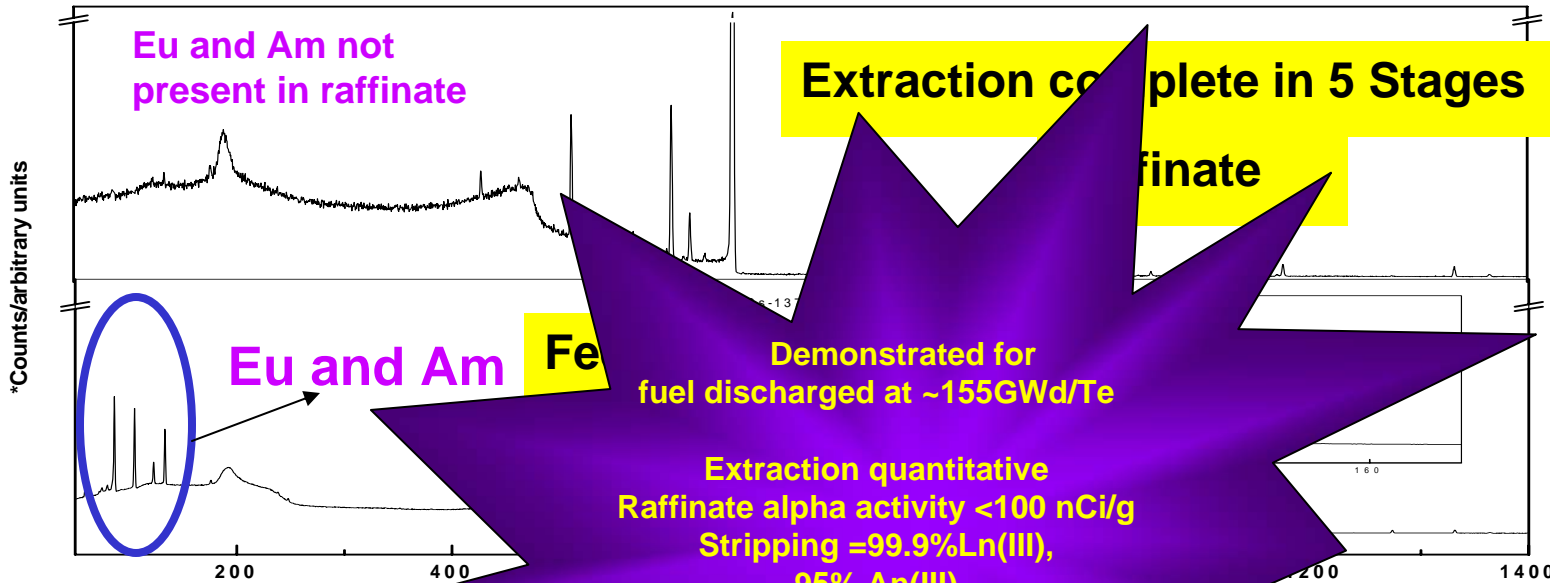




Gamma spectra of the feed (a) and aqueous raffinate (b). \*The data in (a) and (b) are represented in arbitrary units. The enlarged version (40 - 170 keV) of feed is also shown

## Back Extraction in 12 Stages

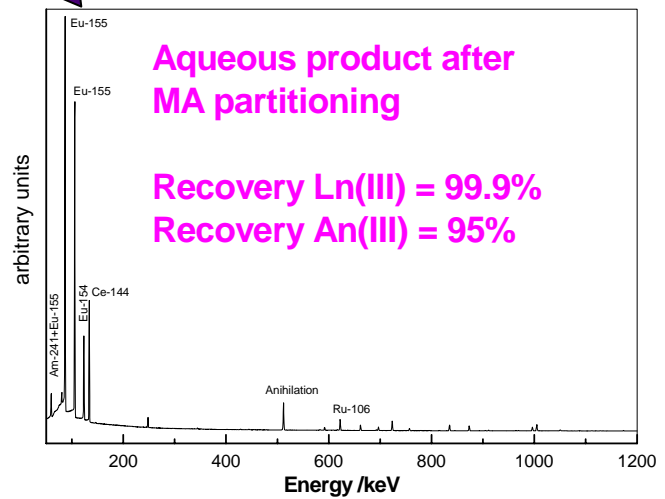
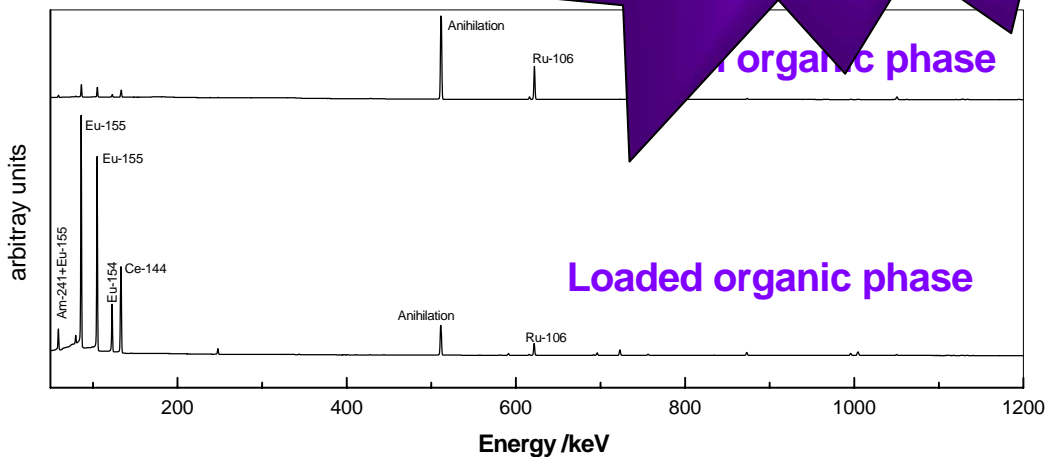




Gamma spectra represented in arbitrary units. Data in (a) and (b) are representative of feed is also shown

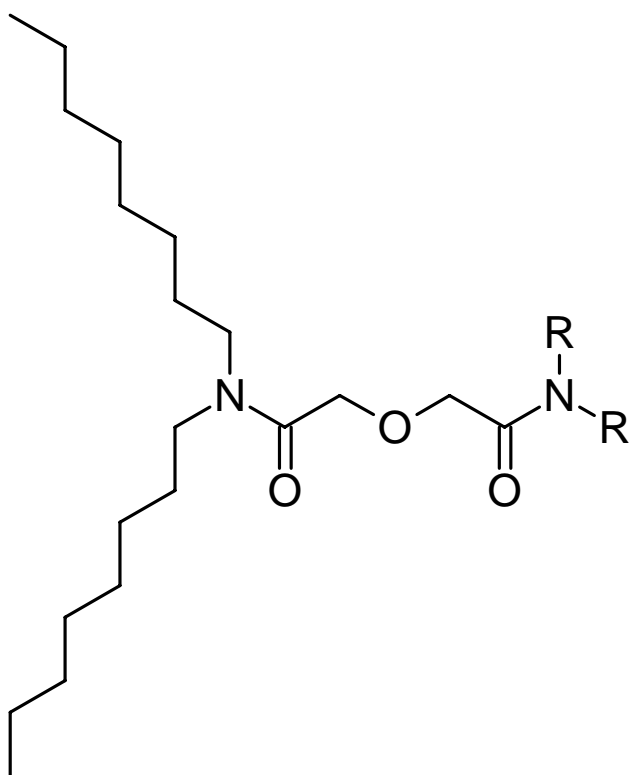
Extraction quantitative  
Raffinate alpha activity <100 nCi/g  
Stripping =99.9%Ln(III),  
95% An(III)

<sup>106</sup>Ru ~25% in lean organic, removed by NaOH+Na<sub>2</sub>CO<sub>3</sub>  
<sup>106</sup>Ru ~10% in product



# Alternate Extractants: Diglycolamides

R = hexyl, C8-C6 – unsymmetrical  
R = octyl, C8-C8 – symmetrical = TODGA  
R = decyl, C8-C10 – unsymmetrical  
R = dodecyl, C8-C12 –unsymmetrical



TODGA and TEHDGA –low solubility in aqueous phase & high distribution ratio for An(III)

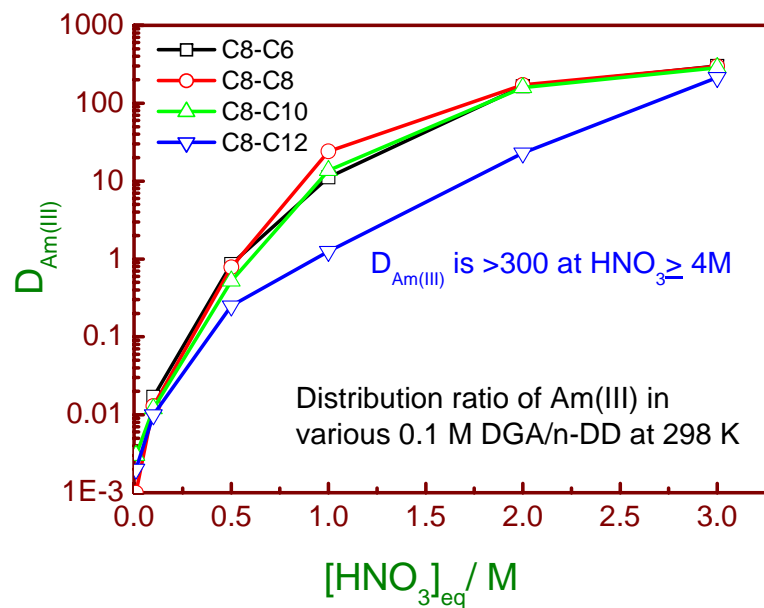
Limitations of Octyl substituents

- Third phase formation with nitric acid and Nd(III)
- Demand phase modifier (0.5 - 1 M)
- Stripping requires complexing agents and large no. of stages
- Low separation factor of Am(III) over Sr(II)

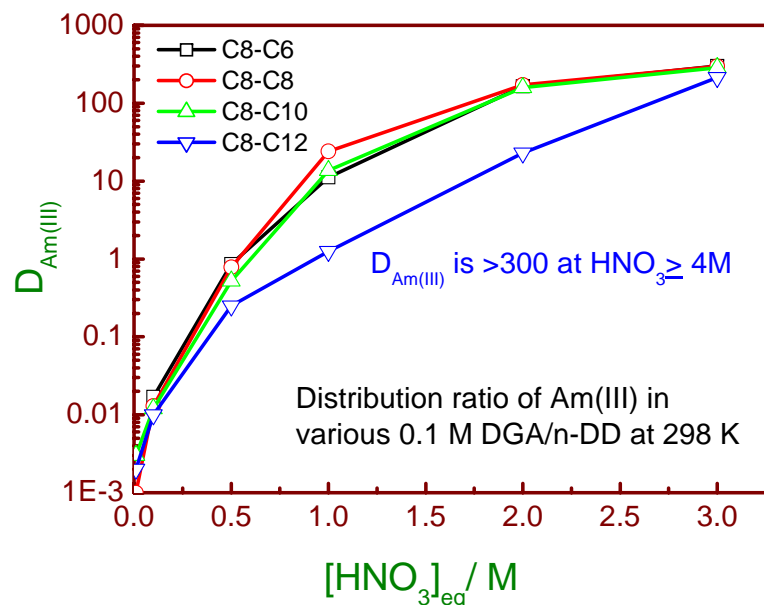
*Increasing the length of the substituent helps w.r.t third phase formation, but reduces Am extraction*

***Solution: Unsymmetrical diglycolamides ?***

# Unsymmetrical diglycolamides: some early results



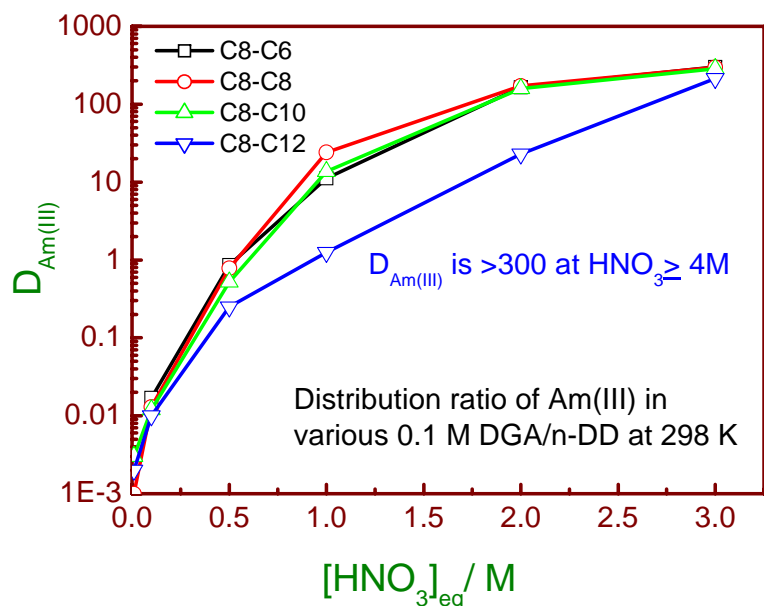
# Unsymmetrical diglycolamides: some early results



Third phase formation of nitric acid (M), 298 K

DGA	[HNO <sub>3</sub> ] <sub>ini</sub>	LOC	CAC
C8-C6	3.6	0.08	3.19
C8-C8	6	0.18	5.14
C8-C10	7	0.20	5.6
C8-C12	12.1	0.28	9.3

# Unsymmetrical diglycolamides: some early results



## Third phase formation of Nd(III) at 298 K

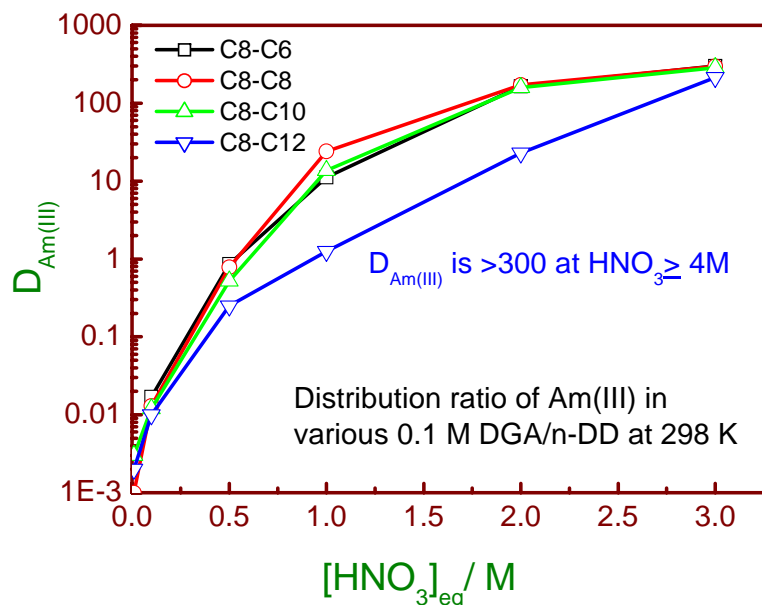
DGA	3 M HNO <sub>3</sub>		4 M HNO <sub>3</sub>		5 M HNO <sub>3</sub>	
	[Nd] <sub>ini</sub> mM	LOC mM	[Nd] <sub>ini</sub> mM	LOC mM	[Nd] <sub>ini</sub> mM	LOC mM
C8-C6	Forms third phase even with trace levels trivalents at $\geq 3$ M HNO <sub>3</sub>					
C8-C8	8	6.4	6	2.4	<1	<1
C8-C10	15	13.2	10	8.1	7	3.5
C8-C12	No third phase even at 600 mM of Nd(III) initial				105	24

## Third phase formation of nitric acid (M), 298 K

DGA	[HNO <sub>3</sub> ] <sub>ini</sub>	LOC	CAC
C8-C6	3.6	0.08	3.19
C8-C8	6	0.18	5.14
C8-C10	7	0.20	5.6
C8-C12	12.1	0.28	9.3



# Unsymmetrical diglycolamides: some early results



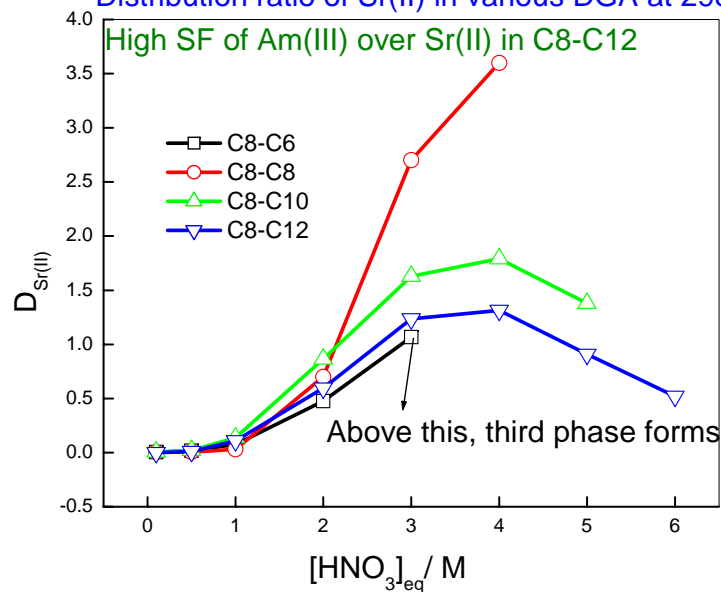
## Third phase formation of Nd(III) at 298 K

DGA	3 M HNO <sub>3</sub>		4 M HNO <sub>3</sub>		5 M HNO <sub>3</sub>	
	[Nd] <sub>ini</sub> mM	LOC mM	[Nd] <sub>ini</sub> mM	LOC mM	[Nd] <sub>ini</sub> mM	LOC mM
C8-C6	Forms third phase even with trace levels trivalent at $\geq 3$ M HNO <sub>3</sub>					
C8-C8	8	6.4	6	2.4	<1	<1
C8-C10	15	13.2	10	8.1	7	3.5
C8-C12	No third phase even at 600 mM of Nd(III) initial				105	24

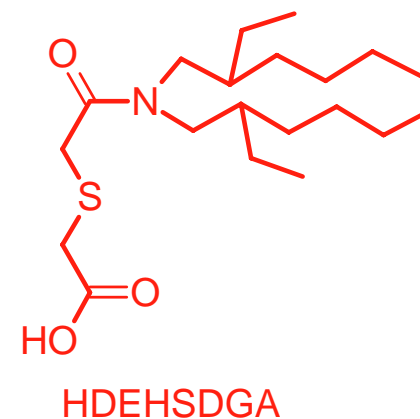
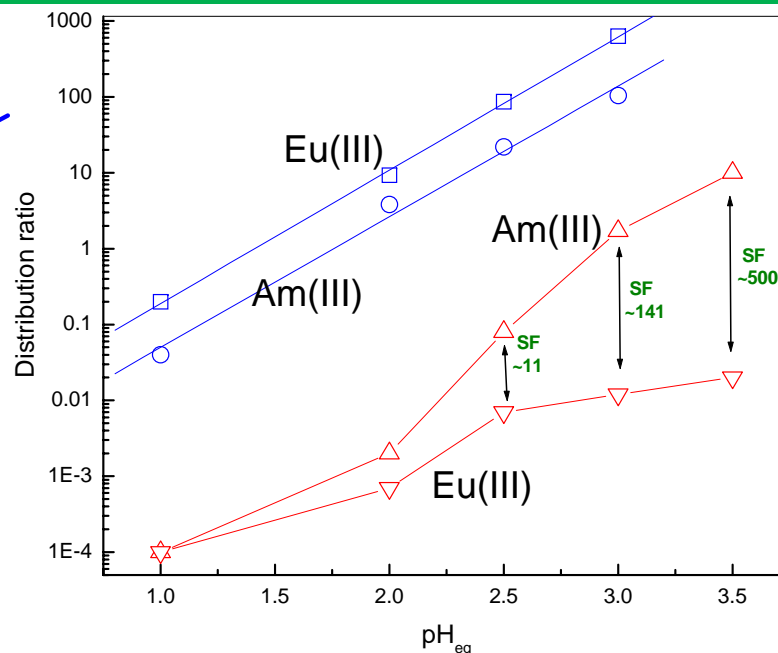
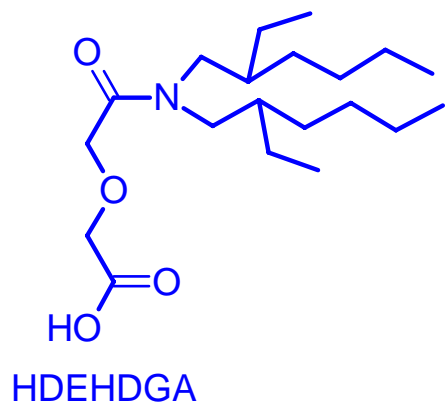
## Third phase formation of nitric acid (M), 298 K

DGA	[HNO <sub>3</sub> ] <sub>ini</sub>	LOC	CAC
C8-C6	3.6	0.08	3.19
C8-C8	6	0.18	5.14
C8-C10	7	0.20	5.6
C8-C12	12.1	0.28	9.3

## Distribution ratio of Sr(II) in various DGA at 298 K

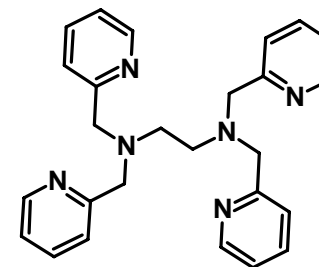


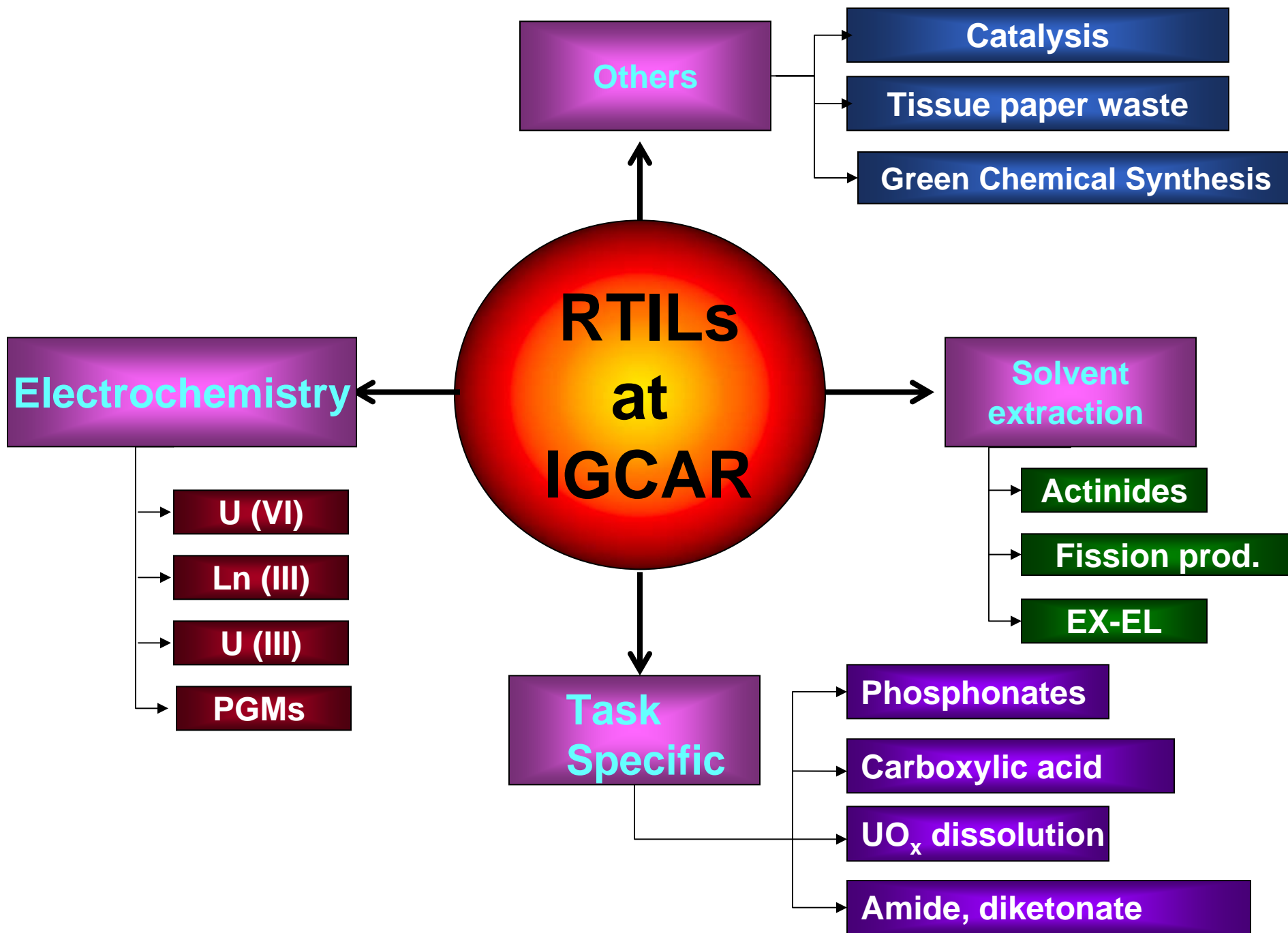
# Diglycolamic acids for Ln(III)/An(III) separation



SF is very high

0.1 M HDEHDGA, Aq. Phase: [DTPA], pH=3				0.3 M HDEHSDGA, Aq. Phase: [HNO <sub>3</sub> ], pH=3			
[DTPA]/ M	$D_{\text{Eu}}$	$D_{\text{Am}}$	SF	[TPEN]/M	$D_{\text{Am}}$	$D_{\text{Eu}}$	SF
0	298	141	2.1	0	0.6	$4.2 \times 10^{-3}$	141
$10^{-5}$	27.6	0.19	145	0.005	0.7	$4.6 \times 10^{-3}$	152
$10^{-4}$	4.9	$6.5 \times 10^{-2}$	75	0.01	1.0	$2.3 \times 10^{-3}$	440
0.001	0.8	$1.7 \times 10^{-2}$	45	0.1	9.8	$3.7 \times 10^{-3}$	2648
0.005	0.2	$2.5 \times 10^{-2}$	10	-	-	-	-





# RTIL as diluent: effect on third phase formation

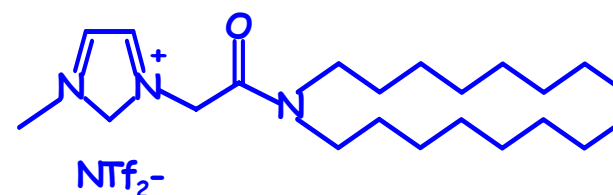
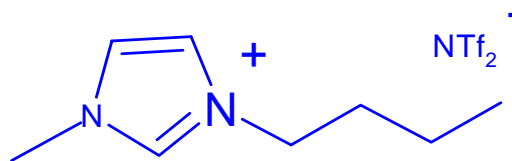
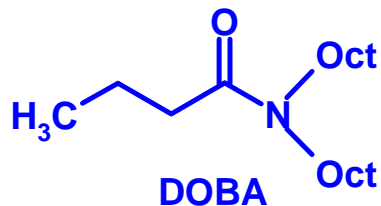
Variation of europium(III) loading in 0.2 M CMPO – 1.2 M TBP/bmimNTf<sub>2</sub> at various initial concentrations.

[Eu(III)] <sub>ini</sub> , mg/ml	Organic loading(mg/ml) at different equilibrium acidities and temperatures					
	1M		3M		5M	
	303K	333K	303K	333K	303K	333K
20	12.1	11.2	12.2	11.2	12.4	10.9
50	16.0	15.0	16.1	14.9	15.7	15.1
100	22.7	18.7	24.2	20.5	21.0	20.0
150	26.2	24.7	25.4	23.3	24.2	23.7
200	32.1	28.8	30.1	29.8	30.5	27.6
250	36.3	35.2	36.3	33.1	34.1	32.6
300	43.2	42.2	38.5	37.7	36.4	34.1

Near solubility limit

No third phase formation using bmimNTf<sub>2</sub>  
Nearly 0.2 M TBP inevitable to avoid crud formation

# DOAImNTf<sub>2</sub>: Unusual Selectivity for Pu(IV) over U(VI)

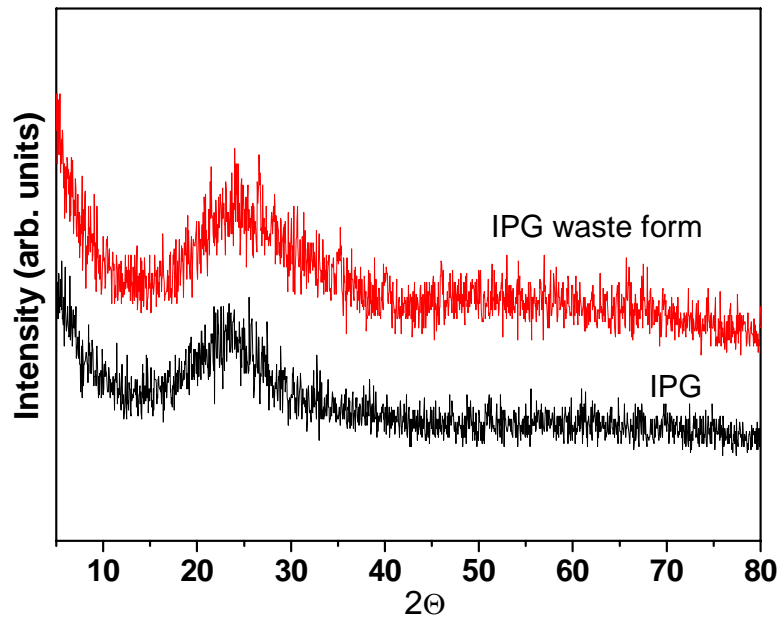


[HNO <sub>3</sub> ] <sub>eq</sub> /M	Distribution ratio in 0.5 M DOBA in C <sub>4</sub> mimNTf <sub>2</sub>		SF = D <sub>Pu(IV)</sub> /D <sub>U(VI)</sub>	Distribution ratio in 0.3 M DOAImNTf <sub>2</sub> / C <sub>4</sub> mimNTf <sub>2</sub>		SF = D <sub>Pu(IV)</sub> /D <sub>U(VI)</sub>
	Pu(IV)	U(VI)		Pu(IV)	U(VI)	
0.5	0.03	0.23	0.13	52	0.015	3466
1	0.05	0.15	0.33	44	0.02	2200
3	1	0.13	7.7	30	0.13	230
4	3	0.15	20	21	0.2	105
5	5	0.4	12.5	20	0.4	50

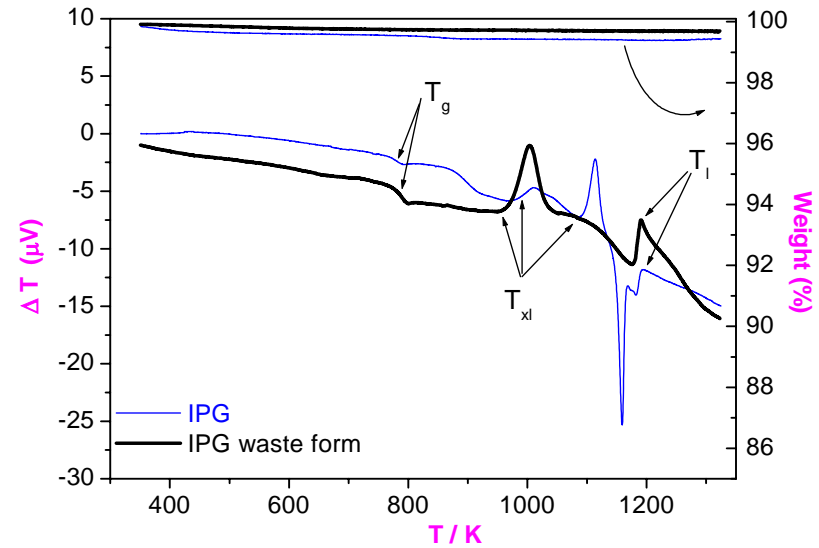
**Amide Functionalised RTIL better than Amide itself; extraction trend also different !**

# Immobilization of FBR waste: Iron Phosphate Glass (IPG)

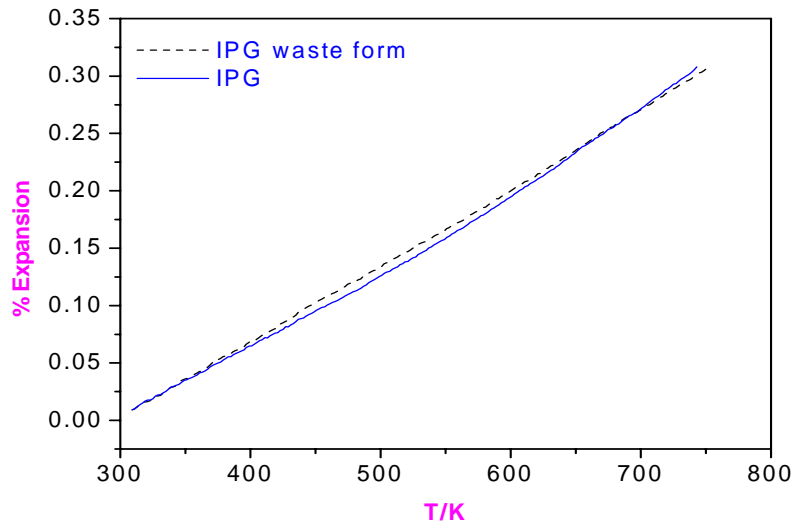
- **HLW of FBR is rich in rare earths and noble metals, not amenable for immobilisation in conventional borosilicate glass (BSG)**
- **Iron phosphate glass (IPG) is a suitable alternate matrix for the high level waste from FRFR because of the ease of glass formation, high percentage of loading achievable, lower homogenization time, better chemical durability, and higher density as compared to BSG**
- **IPG waste form containing simulated FBR HLW was synthesised and characterised at IGCAR using a number of techniques**



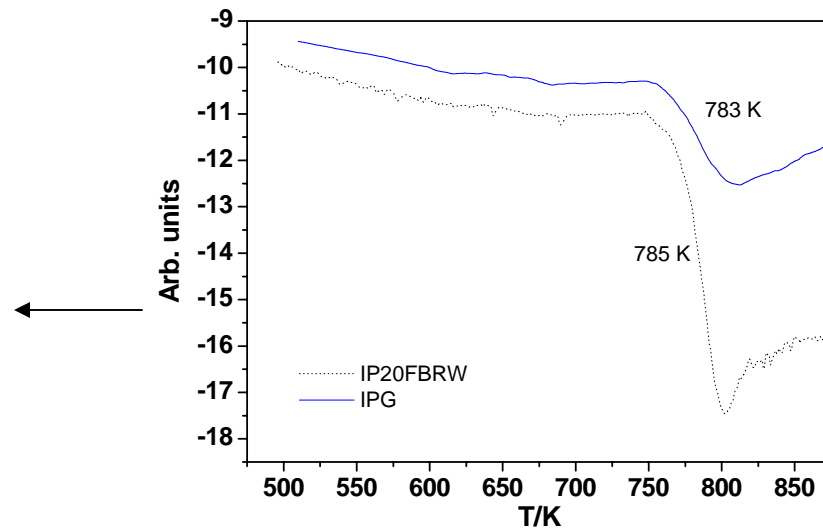
XRD pattern of the IPG and its waste form



TG/DTA of IPG and its waste form



Linear thermal expansion behaviour of IPG and its waste form



DSC curve of IPG and its waste form

## Comparison of Iron Phosphate Glass with Typical Borosilicate Glass and BSG

Properties	IPG (our work)	IPG- 20wt % FR SHLLW (our work)	BSG- 21 wt % BWR waste [29]	BSG [31]
Glass transition T (K)	783	785	809*	818
Initial crystallization T (K)	968	950	-	882
Liquidus T (K)	1198	1191	-	1160
Density (g/cc)	2.9	3.1	3.0	-
Thermal Conductivity ( $\text{Wm}^{-1}\text{K}^{-1}$ )	1.2 [30]	-	0.95	-
Leach rate ( $\text{gcm}^{-2}\text{day}^{-1}$ )	$2.4 \times 10^{-8}$ [30]	-	$4.2 \times 10^{-6}$	-

\* Softening temperature measured by dilatometry



# Immobilisation of (simulated) Fast Reactor waste in Iron Phosphate Glass

Properties of IPG waste form containing 20 wt % simulated FR waste compared with that of pristine IPG

Characterisation techniques and salient results:

- ❖ **X-ray diffraction** : IPG and IPG waste form are amorphous
- ❖ **TGA-DTA and DSC** : Characteristic temperatures like glass transition temperature, initial crystallization temperature and liquidus temperature indicate that **glass forming ability** and **glass stability** of IPG waste form are similar to that of IPG
- ❖ Thermal expansion measurements by **dilatometry** showed that the expansion behaviour of IPG was not altered by the addition of 20 wt % of waste

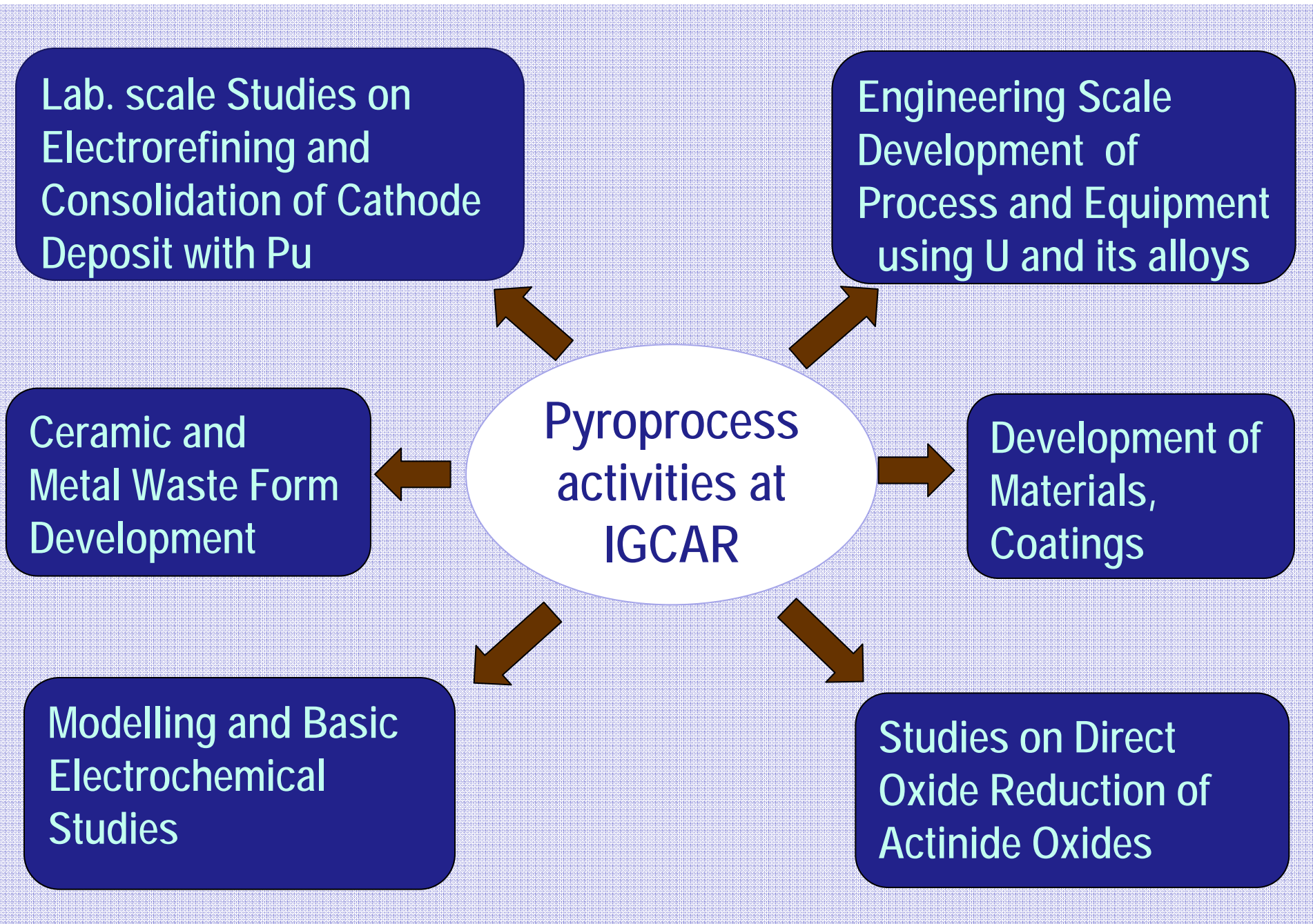
**Conclusion:** Good glass forming characteristics and similar thermal behaviour of waste form with IPG indicate that IPG is an attractive candidate as the matrix for FR waste

# Immobilization of Cesium in IPG

IPG characterised as a function of cesium loading

- ❖ Up to 49 wt %  $\text{Cs}_2\text{O}$  loading, IPG remains amorphous, and shows low volatilization ( $< 0.5$  wt % at 1263 K / 4h)
- ❖  $T_g$  of 29 wt %  $\text{Cs}_2\text{O}$  loaded is 60°C higher than 49 wt %  $\text{Cs}_2\text{O}$  loaded IPG; glass forming characteristics (CCR) are better for 49 wt %  $\text{Cs}_2\text{O}$  loaded IPG
- ❖ Mössbauer studies:  $\text{Fe}^{3+}/\text{Fe}$  is  $> 0.95$  for all glasses (49 wt %  $\text{Cs}_2\text{O}$  : 0.98) : an added advantage since  $\text{Fe}^{3+}$  acts as a glass former in IPG
- ❖ Structural (Infrared and Raman spectroscopy) and crystallization studies clearly indicate the pyrophosphate linkage in IPG and cesium loaded IPG

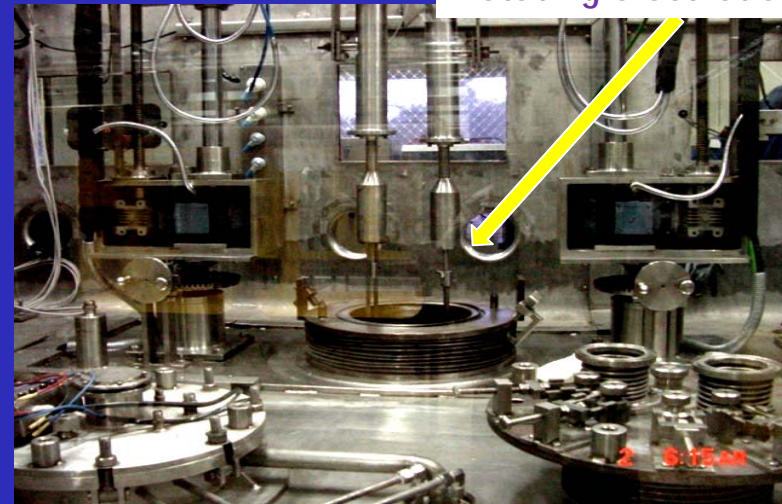
**Conclusion:** Good glass forming characteristics, high loading (49 wt %  $\text{Cs}_2\text{O}$ ) with low volatilization indicate that IPG is a promising matrix to immobilise Cs-137 for use in medical applications



***Pyroprocess under development to cater to the metallic fuels programme***



Argon atmosphere Containment Box



Rotating electrodes

Electrorefining vessel



U deposit on solid cathode



Distillation furnace chamber



U metal ingot

*Engineering Scale Facility for Pyroprocess Studies*

## OTHER STUDIES

**Ambient Temperature Electrorefiner (ATER)** for validation of mechanical engineering design and automation and remote handling concepts, including cathode configurations

Operational experience of ATER to be used for designing the **High Temperature Electrorefiner (HTER)** of 10 kg/ batch capacity

**Development of actinide draw down process**

**Direct Oxide Reduction:** Electroreduction demonstrated on 100 g scale in  $\text{CaCl}_2$  melts

**Modeling :**

Assessment of  $\text{LiCl-UCl}_3$  and  $\text{KCl-UCl}_3$  binary systems using PARROT module of ThermoCalc: Enthalpy of mixing modelled using a modified form of Surrounded Ion Model

Computational modeling of electrorefiner based on diffusion (DIFAC): Code developed to model anodic dissolution of metal alloys, and validated using data on U, Zr, and U-Zr alloys

# Summary

**India is pursuing closed fuel cycle as an important tool for enabling the growth of a sustainable nuclear power programme**

**Fast reactors will be an important component of the nuclear energy mix in India in the coming decades**

**Chemistry aspects of fast reactor fuel cycle, and especially the back end, are being addressed comprehensively**

**New innovative extraction systems are under development for actinide and fission product recovery**

**As part of the long term development of metal fuelled FBRs, pyrochemical reprocessing is under development**



Thank You